Journal of Virology

Intranasal Treatment with Poly(I·C) Protects Aged Mice from Lethal Respiratory Virus Infections

Jincun Zhao, Christine Wohlford-Lenane, Jingxian Zhao, Erica Fleming, Thomas E. Lane, Paul B. McCray Jr. and Stanley Perlman

J. Virol. **2012, 86(21):11416. DOI: 10.1128/JVI.01410-12. Published Ahead of Print 22 August 2012.**

JVI Journals.ASM.org

Intranasal Treatment with Poly(I·C) Protects Aged Mice from Lethal Respiratory Virus Infections

Jincun Zhao,[a] Christine Wohlford-Lenane,[b] Jingxian Zhao,[a,c] Erica Fleming,[a] Thomas E. Lane,[d] Paul B. McCray, Jr.,[a,b] and Stanley Perlman[a,b]

Departments of Microbiology[a] and Pediatrics,[b] University of Iowa, Iowa City, Iowa, USA; Institute for Tissue Transplantation and Immunology, Jinan University, Guangzhou, China[c]; and Department of Molecular Biology and Biochemistry, University of California at Irvine, Irvine, California, USA[d]

In the 2002-2003 severe acute respiratory syndrome coronavirus (SARS-CoV) epidemic, no patients under 24 years of age died, while mortality was greater than 50% in those over 65 years. Greater than 90% of all deaths from influenza A virus (IAV) occur in the elderly (>65 years of age). To address this age-related susceptibility to SARS-CoV and IAV, we infected C57BL/6 (B6) mice with mouse-adapted SARS-CoV (MA15) or IAV (PR8), both of which cause severe disease in aged mice. Intranasal pretreatment of aged mice with poly(I·C) (a TLR3 agonist) and, to a lesser extent, CpG, R848, or lipopolysaccharide (TLR9, TLR7/8, or TLR4 agonists), provided a high level of protection [90% to 100% survival rate after poly(I·C) treatment] against lethal MA15 or IAV challenge and reduced pathological changes and virus loads in the lungs at early times after infection. Poly(I·C) pretreatment upregulated beta interferon (IFN-β), IFN-γ, IL-1β, and tumor necrosis factor (TNF) gene expression in the lungs. Intranasal pretreatment with IFN-β or IFN-γ but not IL-1β or TNF also protected aged mice, consistent with the notion that poly(I·C) pretreatment functioned, at least in part, by inducing IFN-β and IFN-γ. We also identified a potential cellular target for poly(I·C) by showing that treatment inhibited virus replication in primary human airway epithelial cells. These results suggest that intranasal poly(I·C) should be evaluated as a prophylactic agent in aged individuals at high risk for contracting SARS-CoV or IAV infections.

The severe acute respiratory syndrome (SARS), caused by a novel coronavirus (SARS-CoV), resulted in 10% mortality during the 2002-2003 epidemic (23). This elevated overall mortality resulted in part from a low survival rate (50%) in individuals over 65 years of age. This was in marked contrast to the 100% survival observed in young (<24 years old) infected patients (23). To investigate this age-related increase in mortality, as well as other features of SARS pathogenesis, several animal models have been developed (28). One mouse-adapted strain of SARS-CoV, MA15, is especially useful for pathogenesis studies since it causes severe disease in aged mice of all strains (24). In contrast, 6-week-old C57BL/6 (B6) mice are highly resistant to MA15 (7, 33, 34).

While SARS-CoV causes an especially steep age-dependent increase in mortality, other respiratory viral infections, such as influenza A virus (IAV) and respiratory syncytial virus (RSV), also cause more severe disease in older patients (6, 20, 25, 32). Multiple defects in the innate and adaptive immune responses have been documented in aged individuals and experimental animals. Dysregulated innate immune responses contributed to severe disease in humans infected with SARS-CoV or IAV strains, including H5N1, and also occurs in aged mice and macaques infected with SARS-CoV (2, 4, 25, 27). A well-balanced innate response resulted in robust antibody and T cell responses in infected patients and mice that survive the infection (2).

Prevention of infectious diseases in aged populations has proven difficult, because older individuals often respond poorly to vaccines (12, 14, 19). Thus, alternative prophylactic strategies are required to improve outcomes. Immune responses to respiratory virus infections must also overcome the naturally inhibitory milieu of the lungs. Some aspects of this inhibitory milieu are enhanced with aging, contributing to poor responses in aged individuals (5, 10, 33). Thus, we reasoned that interventions that countered the anti-inflammatory milieu in aged animals would result in better innate and, ultimately, antivirus T cell and antibody responses. TLR agonists, such as poly(I·C) and CpG, signal through MyD88- and TRIF-dependent pathways to induce expression of interferons and proinflammatory cytokines and chemokines. Here, we show that mortality in 12- to 22-month-old mice infected with SARS-CoV or IAV was reduced from 80 to 100% to 0 to 10% by treatment with a TLR3 agonist, poly(I·C), with concomitant increased expression of interferon (IFN) and other proinflammatory molecules, enhanced T cell responses, and more rapid virus clearance.

MATERIALS AND METHODS

Mice, virus, and cells. Specific-pathogen-free C57BL/6 (B6) mice with ages ranging from 12 to 24 months were purchased from the National Cancer Institute and National Institute on Aging. Mice were maintained in the animal care facility at the University of Iowa. All protocols were approved by the University of Iowa Institutional Animal Care and Use Committee. Mouse-adapted SARS-CoV (MA15) was a kind gift from Kanta Subbarao (NIH, Bethesda, MD) (24). Mouse-adapted IAV A/PR/8/34 was grown in the allantoic fluid of 10-day-old embryonated chicken eggs for 2 days at 37°C as previously described (16). Vero E6 cells and MDCK cells were grown as described previously (33).

Virus infection and titration. B6 mice were lightly anesthetized with isoflurane and infected intranasally with 1×10^5 PFU of SARS-CoV or 1,066 tissue culture infectious doses ($TCID_{50}$) of IAV in a total volume of

Received 6 June 2012 Accepted 16 August 2012
Published ahead of print 22 August 2012
Address correspondence to Jincun Zhao, jincun-zhao@uiowa.edu, or Stanley Perlman, stanley-perlman@uiowa.edu.

doi:10.1128/JVI.01410-12

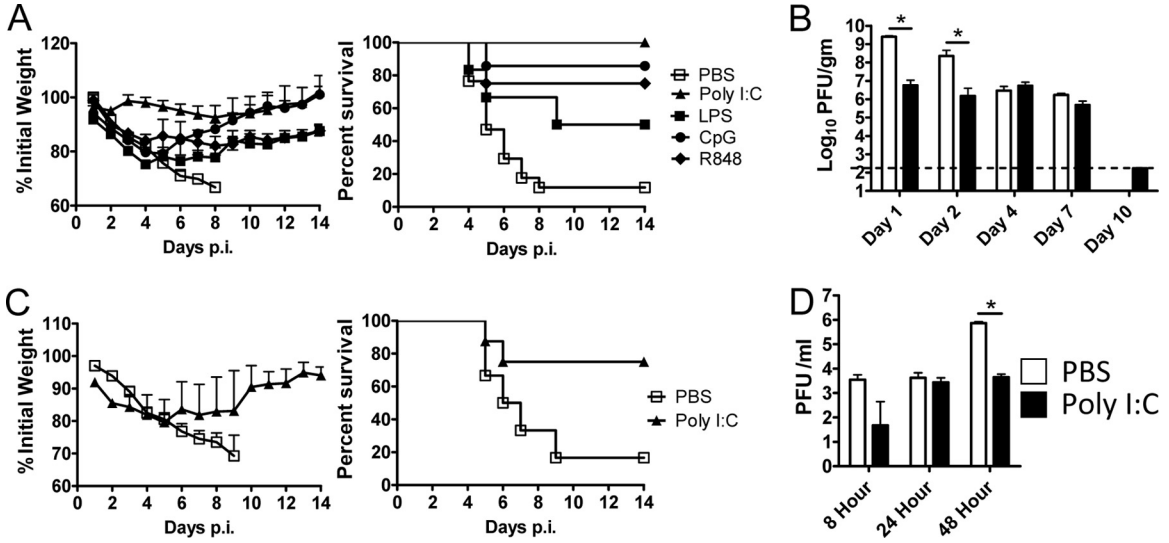

FIG 1 Effect of TLR agonist treatments on weight loss, virus titers, mortality, and histological changes in MA15-infected aged B6 mice. (A) Twelve-month-old B6 mice were treated with 20 μg poly(I·C), 100 μg CpG, 5 μg LPS, 10 μg R848, or PBS 6 h before intranasal infection with 1×10^5 PFU MA15 virus. Weight loss and mortality were monitored daily. $n = 17$ mice in the PBS group, 13 in the poly(I·C) group, 6 in the LPS group, 7 in the CpG group, and 8 in R848 group. (B) To obtain virus titers, lungs were homogenized and virus titers determined on Vero E6 cells. Titers are expressed as PFU/g tissue. $n = 4$ mice/group/time point. Data are representative of 2 independent experiments. *, $P < 0.05$. (C) Twenty-two-month-old B6 mice were treated with 20 μg poly(I·C) or PBS 6 h prior to infection with 1×10^5 PFU MA15 virus. $n = 7$ mice in the PBS group and 8 mice in the poly(I·C) group. (D) Human polarized airway epithelial cells were treated with poly(I·C) (1 μg/ml) and infected with MA15 as described in Materials and Methods. Virus titers were determined by plaque assay. Data are representative of 3 independent experiments.

50 μl Dulbecco's modified Eagle medium (DMEM). Mice were monitored daily for morbidity and mortality. All work with SARS-CoV was conducted in the University of Iowa biosafety level 3 (BSL3) laboratory. To obtain SARS-CoV and IAV titers, lungs were removed into phosphate-buffered saline (PBS) and homogenized using a manual homogenizer. Virus titers were determined on Vero E6 cells or MDCK cells as previously described (16, 35). Viral titers are expressed as PFU/g tissue for SARS-CoV and $TCID_{50}$/ml for IAV.

TLR agonist and cytokine treatments. TLR agonists poly(I·C), CpG, and imidazoquinoline (R848) were purchased from Invivogen (San Diego, CA). Lipopolysaccharide (LPS; Alexis Biochemicals, Farmingdale, NY), beta interferon (IFN-β; PBL, Piscataway, NJ), interleukin-1β (IL-1β), tumor necrosis factor (TNF), IFN-γ, IL-6, IL-12 (R&D Systems, McKinley Place, NE), and granulocyte-macrophage colony-stimulating factor (GM-CSF) (BD Bioscience, San Jose, CA) were purchased. At the indicated time points, mice were lightly anesthetized with isoflurane and treated with various doses of TLR agonists and cytokines intranasally in a total volume of 50 μl PBS. In some experiments, 80 μg poly(I·C) was delivered by the intraperitoneal (i.p.), subcutaneous (s.c.), or intravenous (i.v.) route in 200 μl PBS.

Epithelial cell culture and infection. Well-differentiated primary cultures of human airway epithelia were prepared from bronchial cells and maintained at the air-liquid interface on collagen-coated porous filters as described previously (11). Cells were then grown in serum-free media for 72 h. Poly(I·C) (1 μg/ml) was then applied both apically and basolaterally to cells 4 h prior to MA15 infection. After 4 h, poly(I·C) was removed from the apical surface and cells were washed and infected with MA15 (multiplicity of infection [MOI], 0.1) for 1 h. Samples were collected at the indicated time points and analyzed for infectious virus by plaque assay.

Histology. Animals were anesthetized and transcardially perfused with PBS followed by zinc formalin. Lungs were removed, fixed in zinc formalin, and paraffin embedded. Sections were stained with hematoxylin and eosin.

Preparation of cells from lungs and draining lymph nodes. Mice were sacrificed at the indicated time points. The lung vascular bed was flushed via the right ventricle with 5 ml PBS, and lungs and draining lymph nodes (DLN) were then removed. Lungs were cut into small pieces and digested in Hanks buffered salt solution (HBSS) containing 2% fetal calf serum (FCS), 25 mM HEPES, 1 mg/ml collagenase D (Roche), and 0.1 mg/ml DNase (Roche) for 30 min at room temperature. Lymph nodes were minced and pressed though a wire screen. Single-cell suspensions were prepared. Live cells were enumerated by 0.2% trypan blue exclusion.

***In situ* CFSE staining.** Carboxyfluorescein succinimidyl ester (CFSE; Molecular Probes) was diluted in DMEM to a concentration of 8 mM and then administered intranasally (i.n.; 50 μl/mouse) 6 h before infection following anesthesia with isoflurane.

Peptide stimulation and tetramer staining. SARS-CoV-specific peptides S436 (HNYKYRYL) and S525 (VNFNFNGL) were synthesized by BioSynthesis Inc. (Lewisville, TX). $H2K^b$/S436 and $H2K^b$/S525 tetramers were obtained from the National Institute of Allergy and Infectious Disease MHC Tetramer Core Facility (Atlanta, GA). For tetramer staining, cells were stained for 30 min at 4°C. Cells were then stained for other surface markers. For intracellular cytokine staining (ICS), 1×10^6 cells/well were cultured in 96-well dishes at 37°C for 5 to 6 h in the presence of brefeldin A (BD Biosciences). Cells were then labeled for cell surface markers, fixed/permeabilized with Cytofix/Cytoperm solution (BD Biosciences), and labeled with anti-IFN-γ antibody.

Antibodies and flow cytometry. The following monoclonal antibodies were used: rat anti-mouse CD4 (RM4-5), rat anti-mouse CD8α (53-6.7), rat anti-mouse CD11b (M1/70), hamster anti-mouse CD11c (HL3), rat anti-mouse CD16/32 (2.4G2), rat anti-mouse Siglec F (E50-2440), rat anti-mouse Ly-6C (AL-21), rat anti-mouse Ly-6G (1A8), and rat anti-mouse CD45 (30-F11) (all from BD Bioscience); rat anti-mouse IFN-γ (XMG1.2; from eBioscience); and rat anti-mouse I-A/I-E (M5/114.15.2; from Biolegend). For surface staining, 10^6 cells were blocked with 1 μg anti-CD16/32 antibody and 1% rat serum and stained with the indicated antibodies at 4°C. All flow cytometry data were acquired on a BD FACSCalibur and were analyzed using FlowJo software (Tree Star, Inc.).

Cytokine and chemokine RNA levels measured by qRT-PCR. RNA was extracted from infected lungs using TRIzol (Invitrogen) and used in

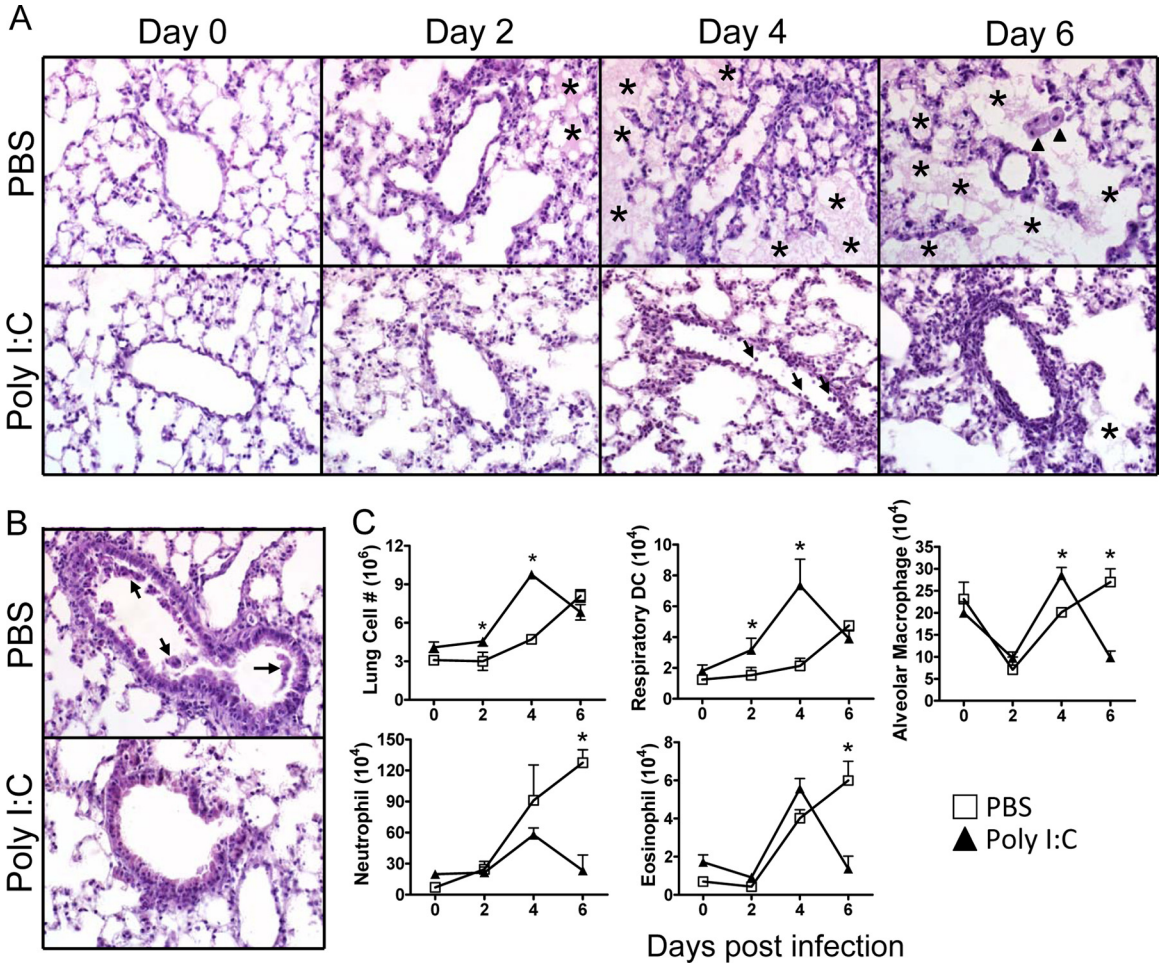

FIG 2 Poly(I·C) treatment reduces pulmonary edema and accelerates inflammatory cell infiltration into SARS-CoV-infected lungs. Twelve-month-old B6 mice were treated with 20 μg poly(I·C) or PBS 6 h before intranasal infection with 1×10^5 PFU MA15 virus. (A) Lungs were removed at the indicated time points p.i., fixed in zinc formalin, and embedded in paraffin. Sections were stained with hematoxylin and eosin. Asterisks indicate edema, arrowhead shows a foamy macrophage, and arrows indicate marginating cells. (B) Necrotic debris (arrows) was detected at day 2 p.i. in the airways of PBS-treated mice. (C) Lungs were harvested at the indicated time points, and after enzyme digestion, single-cell suspensions were acquired. Total numbers of lung cells, rDCs ($CD11c^+$ $MHCII^+$ $SiglecF^-$), alveolar macrophages ($CD11c^+$ $MHCII^{+/-}$ $SiglecF^+$), eosinophils ($CD45^+$ $CD11c^{+/-}$ $SiglecF^+$), and neutrophils ($CD11b^+$ $Ly6C^+$ $Ly6G^+$) in the lung are shown. Data are representative of 2 independent experiments, $n = 4$ mice/group/time point. *, $P < 0.05$.

quantitative reverse transcription-PCRs (qRT-PCRs) (33). Specific primer sets used for assaying cytokine and housekeeping gene expression were previously described (36).

Statistical analysis. A Student's *t* test was used to analyze differences in mean values between groups. All results are expressed as means ± standard errors of the means (SEM). *P* values of <0.05 were considered statistically significant.

RESULTS

Poly(I·C) treatment protects 12- and 22-month-old B6 mice from lethal SARS-CoV infection. While 6-week-old B6 mice are resistant to infection with 10^5 PFU of SARS-CoV (34), mortality in 12- to 22-month-old B6 mice infected with as little as 10^4 PFU of SARS-CoV was 80 to 100%, and all mice developed histological evidence of severe pneumonia (25, 33). For the experiments described below, we infected aged mice with a supralethal dose, 10^5 PFU. To determine if immune activation with TLR agonists was protective, we treated mice with agonists for TLR3 (poly(I·C), TLR4 (LPS), TLR7/8 (R484), and TLR9 (CpG) and then infected them with SARS-CoV. Treatment with agonists for TRL3, TLR7/8, and TLR9 all increased survival, but only poly(I·C) was completely protective (Fig. 1A). Of note, mice that received poly(I·C) in the absence of infection exhibited no overt signs of clinical disease (weight loss, hunching, ruffled fur, or difficulty breathing). Consistent with improved outcomes, virus titers at days 1 and 2 postinfection (p.i.) were significantly reduced by poly(I·C) treatment, with complete clearance by day 10 p.i. (Fig. 1B). Twenty-two-month-old mice are highly susceptible to many respiratory virus infections, including SARS-CoV and IAV (5, 31, 33). Remarkably, poly(I·C) pretreatment was protective in 22-month-old mice infected with SARS-CoV (Fig. 1C).

Poly(I·C) inhibits virus replication in primary human airway epithelial cells. Airway and alveolar epithelial lung cells are major targets for SARS-CoV in both infected patients and mice infected with strain MA15 (9, 21, 24). We analyzed the effect of poly(I·C) on virus replication in lung cells using human airway epithelial cells (HAE). For these experiments, we infected primary HAE

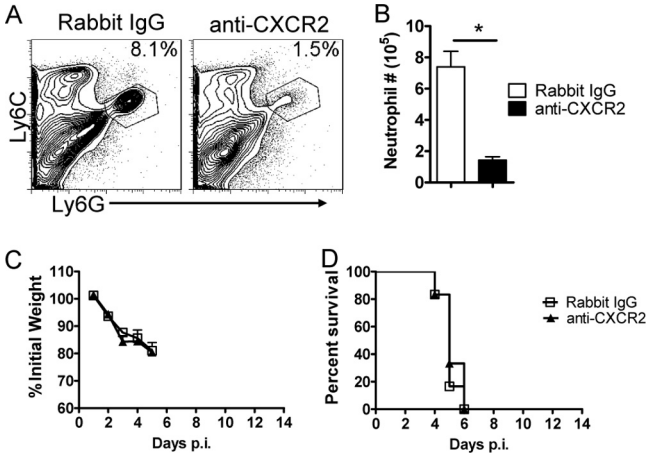

FIG 3 Blocking neutrophil migration to the lungs did not protect 12-month-old mice from lethal SARS-CoV. Twelve-month-old mice were treated with 250 μg rabbit anti-CXCR2 polyclonal antibodies i.p. at days −3 and 0 and at day 3 after intranasal infection with 1×10^5 PFU MA15 virus. Lung cells were harvested 2 days after SARS-CoV infection. Neutrophil frequency (A) and numbers (B) are shown. Data are representative of 3 independent experiments. *, $P < 0.05$. Weight loss (C) and mortality (D) were monitored daily. $n = 6$ mice in rabbit IgG and anti-CXCR2 groups.

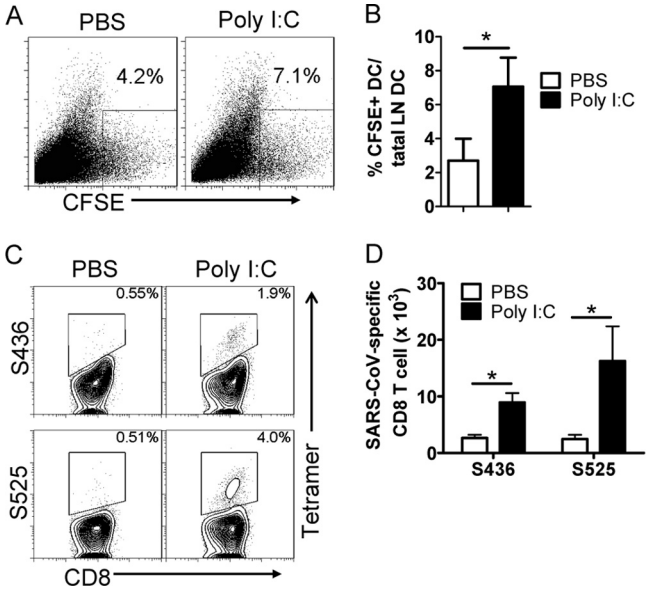

FIG 4 Poly(I·C) treatment enhances rDC migration and T cell responses in the lungs of aged mice. (A and B) Twelve-month-old mice were treated with poly(I·C) or PBS 2 h before intranasal inoculation of 50 μl 8 mM CFSE. Four h after CFSE instillation, mice were infected with 1×10^5 PFU MA15 virus. At 18 h p.i., single-cell suspensions were prepared from lung DLNs and gated for CD11c and MHC-II expression by flow cytometry. The values represent the percentage of $CFSE^+$ cells within the $CD11c^+$ $MHC\text{-}II^+$ DC population. (B and D) Lung cells were harvested from 12-month-old B6 mice 6 days after SARS-CoV infection. Tetramer staining for CD8 T cell epitopes S436 and S525 is shown. $n = 4$ mice/group/time point. Data are representative of 3 independent experiments.

from four donors with SARS-CoV and monitored virus titers in the presence or absence of poly(I·C). As shown in Fig. 1D, poly(I·C) reduced virus titers by 100-fold after 48 h ($P < 0.005$), suggesting that airway epithelial cells are a target for poly(I·C) during the infection.

Poly(I·C) treatment reduces pulmonary edema and accelerates inflammatory cell infiltration into SARS-CoV-infected lungs. Aged mice infected with MA15 develop severe pneumonia and acute lung injury (ALI) as detected by histological examination (25, 33). To determine whether poly(I·C) treatment reversed pathological changes consistent with ALI, we analyzed the lungs of poly(I·C)-treated and control 12-month-old mice at days 2, 4, and 6 p.i. (Fig. 2A). We observed striking differences between PBS- and poly(I·C)-treated infected lungs (Fig. 2A). At day 2 p.i., there was evidence of early edema formation only in the PBS-treated samples. Epithelial cell necrosis and airway debris were present in both groups but were more extensive in the PBS-treated animals (Fig. 2B). At days 4 and 6, we detected perivascular/peribronchial cellular infiltration in the poly(I·C)-treated mice and, to a minimal extent, in the PBS-treated mice. Conversely, protein-rich edema fluid was present only in the PBS-treated animals at day 4 p.i. By day 6 p.i., we observed widespread edema formation and macrophages, some containing cellular debris (arrow), and other inflammatory cells in PBS-treated mice that survived the infection; some edema was observed at this time p.i. in the poly(I·C)-treated mice, even though mice had no signs of clinical illness.

To further quantify the cellular infiltrate in PBS- and poly(I·C)-treated mice, we analyzed lung-derived inflammatory cells by flow cytometry (Fig. 2C). In agreement with the histological findings shown in Fig. 2A and B, treatment with poly(I·C) resulted in increased numbers of total infiltrating lung cells at days 2 and 4 p.i. Respiratory dendritic cells (rDC) and alveolar macrophages were specifically increased at these early times p.i. in poly(I·C)-treated mice. In contrast, numbers of neutrophils and eosinophils were equivalent at day 2 and 4 p.i. but decreased in poly(I·C)-treated mice by day 6 p.i. Since neutrophils may contribute to lung damage, we assessed their role by treating control mice with antibody to CXCR2 (8), a chemokine receptor required for neutrophil ingress into sites of inflammation. Antibody treatment prevented neutrophil infiltration into the infected lungs but had no effect on morbidity or mortality (Fig. 3).

We showed previously that rDC migration to draining lymph nodes (DLN) was impaired in SARS-CoV-infected 12-month-old mice. A consequence of deficient rDC migration was a greatly reduced T cell response in the lungs (33). Reversal of the rDC migration defect and subsequent normalized antivirus T cell response correlated with improved outcomes. To determine whether poly(I·C) augmented rDC migration to DLN, we treated mice intranasally with CFSE. Poly(I·C) treatment resulted in increased rDC migration to draining lymph nodes (Fig. 4A and B). Virus-specific T cell responses in infected lungs were also increased, as measured using major histocompatibility complex class I (MHC-I)/tetramers specific for SARS-CoV CD8 T cell epitopes (Fig. 4C and D).

Poly(I·C) treatment results in earlier expression of IFN-associated molecule expression in SARS-CoV-infected mice. Treatment with poly(I·C) at 6 or 18 h prior to infection resulted in earlier expression of several proinflammatory molecules, including IFN-β, IFN-γ, RIG-I, MDA-5, and Stat1, which contribute to an enhanced antiviral state in the lung and, in conjunction with molecules such as TNF and IL-1β, augment activation and infiltration of immune cells (Fig. 5). Genes encoding protein kinase R (PKR) and 2′-5′-oligoadenylate synthetase 1 (OAS), two interfer-

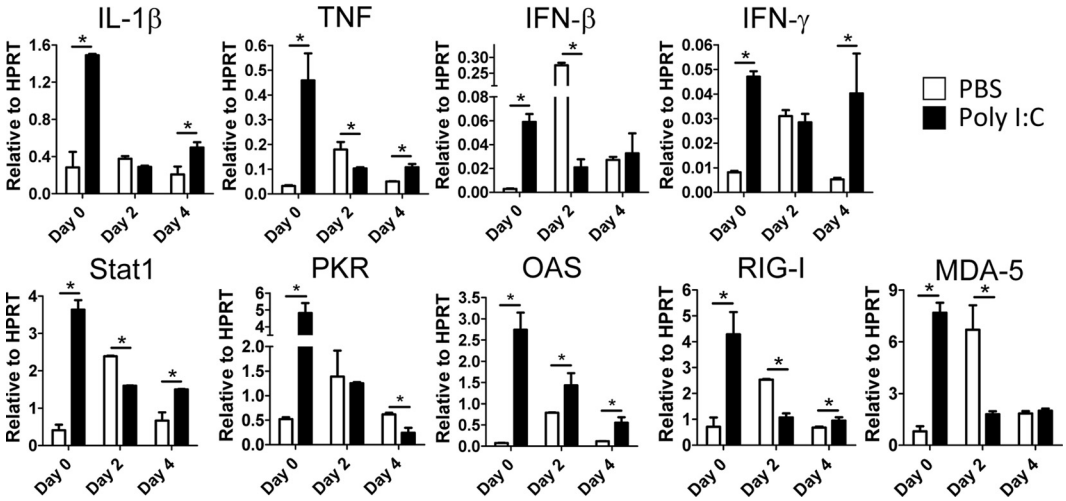

FIG 5 Cytokine and chemokine RNA levels in 12-month-old mice after poly(I·C) treatment and SARS-CoV infection. Mice were treated with poly(I·C) 6 h prior to infection with MA15. RNA was extracted from MA15-infected lungs at the indicated time points and processed as described in Materials and Methods. n = 4 mice/group/experiment. Data are representative of 2 independent experiments. *, $P < 0.05$. HPRT, hypoxanthine phosphoribosyltransferase.

on-stimulated genes with antiviral effects, were also upregulated in poly(I·C)-treated lungs. In the absence of poly(I·C), these molecules were also upregulated but at a later times p.i. (day 2 p.i.). This delay in expression resulted in a response that was too late to inhibit virus replication sufficiently to prevent disease (Fig. 1B).

To begin to determine which of these proinflammatory molecules were most critical for poly(I·C)-mediated protection, we treated SARS-CoV-infected 12-month-old mice intranasally with IFN-γ, IFN-β, IL-1β, IL-6, IL-12, TNF, or GM-CSF, all of which are involved in initiation or propagation of the immune response. Only IFN-β and IFN-γ treatments were protective (Fig. 6A and B). Poly(I·C)-mediated protection was dependent upon both IFN-α/β-dependent and independent pathways, since partial protection occurred in 12-month-old IFNAR mice, which lack the IFN-α/β receptor (Fig. 6C and D). Further, treatment of IFNAR mice with IFN-γ completely protected infected 12-month-old mice from lethal disease. Poly(I·C) functions by binding to TLR3 and to RIG-I and MDA-5, two intracellular helicase sensors (17, 29); as shown in Fig. 6E and F, some of the effects of poly(I·C) were mediated, at least in part, by TLR3, since 50% of the 12-month-old TLR3$^{-/-}$ mice succumbed to the infection.

Poly(I·C) treatment protects 22-month-old mice from lethal IAV infection. To extend these analyses to a second respiratory viral infection, we infected mice with the PR8 strain of IAV. Twenty-two-month-old, but not 12-month-old, mice develop a fatal infection after infection with this strain of IAV (33). We found that treating IAV-infected 22-month-old mice with poly(I·C) 6 h prior to infection was partially protective (approximately 60% survival), and protection was increased to 90% if mice were treated at both 6 and 48 h prior to infection (Fig. 7A). As in SARS-CoV-infected mice, poly(I·C) functioned in part by inducing IFN and other proinflammatory molecules at earlier times p.i. than occurred in PBS-treated mice (Fig. 7B). Treatment with IFN-β completely protected IAV-infected 22-month-old mice from lethal disease, while IFN-γ was approximately 70% protective (Fig. 7A). In previous studies, control of infection within 24 h was shown to be essential for preventing lethal IAV-induced disease (16, 18). As shown in Fig. 7C, poly(I·C) significantly reduced IAV titers at day 1 by nearly 3 logs and by 1 log at day 2 p.i.

As in MA15-infected mice, treatment with poly(I·C) resulted in decreased lung injury (Fig. 8A). Since the tempo of disease in IAV-infected mice is less rapid than that in MA15-infected mice, we obtained samples through day 8 p.i. for histological and flow-cytometric analysis. By day 4 p.i., peribronchial/perivascular infil-

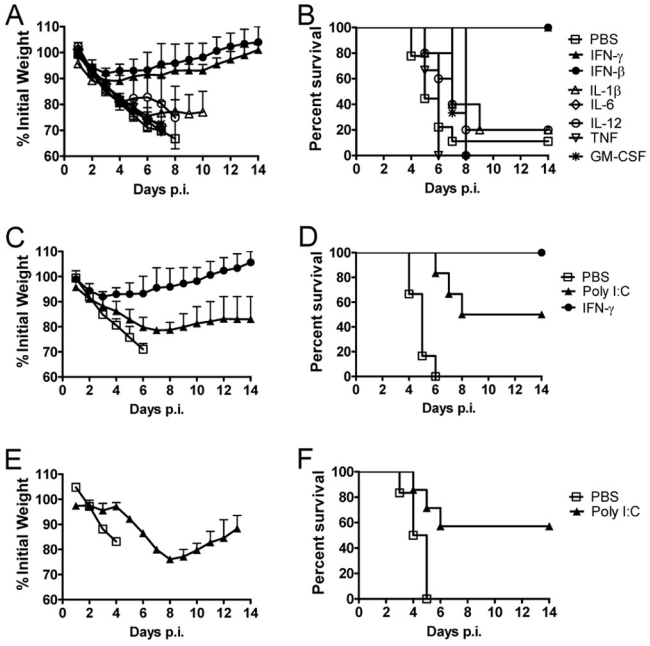

FIG 6 Effect of cytokine or TLR agonist treatments on weight loss and mortality in MA15-infected aged B6, IFNAR$^{-/-}$, and TLR3$^{-/-}$ mice. Twelve-month-old B6 (A and B), 12- to 14-month-old IFNAR$^{-/-}$ (C and D), or 12- to 14-month-old TLR3$^{-/-}$ mice (E and F) were treated with IFN-β (2,000 U), IL-1β (50 ng), TNF (200 ng), IFN-γ (200 ng), IL-6 (50 ng), IL-12 (20 ng), GM-CSF (20 ng), or poly(I·C) (20 μg) 6 h before intranasal infection with 1×10^5 PFU MA15 virus. Weight loss and mortality were monitored daily. For B6 mice, n = 9 in the PBS group, 6 in the IFN-γ group, 6 in the IFN-β group, 10 in the IL-1β group, 8 in the IL-6 group, 10 in the IL-12 group, 6 in the TNF group, and 6 in the GM-CSF group. For IFNAR$^{-/-}$ mice, n = 6 in the PBS group, 6 in the poly(I·C) group, and 6 in the IFN-γ group. For TLR3$^{-/-}$ mice, n = 6 in the PBS group and 7 in the poly(I·C) group.

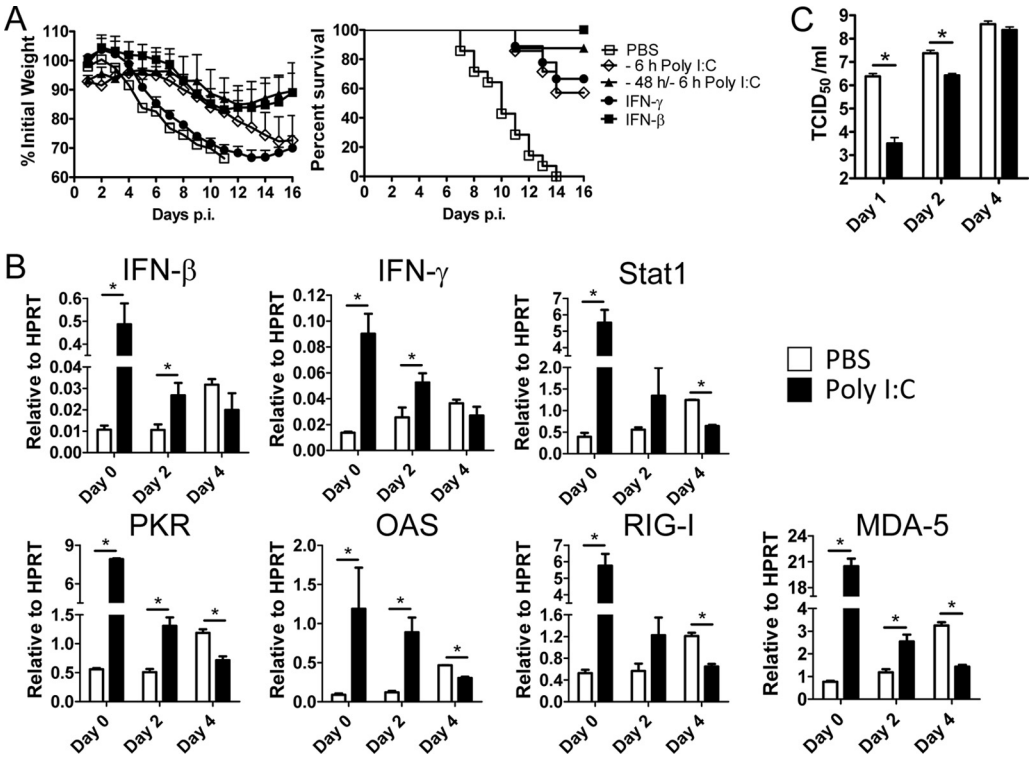

FIG 7 Poly(I·C) or cytokine treatments protect 22-month-old mice from lethal IAV infection. (A) Twenty-two-month-old B6 mice were treated with 20 μg poly(I·C), IFN-β (2,000 U), or IFN-γ (200 ng) 6 h or 6 and 48 h before infection with IAV. Weight loss and mortality were monitored daily. $n = 14$ mice in the PBS group, 7 in the −6-h poly(I·C) group, 8 in the −48-h/−6-h poly(I·C) group, 9 in the IFN-γ group, and 6 in the IFN-β group. (B) Twenty-two-month-old B6 mice were treated with poly(I·C) 48 and 6 h prior to intranasal infection with 1,066 $TCID_{50}$ of IAV. RNA was extracted from lungs at the indicated time points and processed as described in Materials and Methods. $n = 4$ mice/group/experiment. Data are representative of 2 independent experiments. *, $P < 0.05$. (C) For virus titers, lungs were homogenized and titers of virus were determined on MDCK cells. Viral titers are expressed as $TCID_{50}$/ml homogenate. $n = 4$ mice/group/time point. *, $P < 0.05$. Data are representative of 2 independent experiments.

tration and airway obstruction were detected in PBS-treated IAV-infected mice. Disease progressed in these mice so that by day 8, widespread alveolar and airway edema was present. We observed much less edema at day 8 in poly(I·C)-treated mice, consistent with the ameliorated clinical disease observed in these mice (Fig. 7A).

We also quantified the cellular infiltrate in PBS- and poly(I·C)-treated IAV-infected mice by flow cytometry (Fig. 8B). Treatment with poly(I·C) resulted in increased numbers of total infiltrating lung cells at day 4 p.i. compared to PBS-treated IAV-infected mice. Numbers of all cell types (respiratory DCs, alveolar macrophages, neutrophils, and eosinophils) were increased at this time p.i. in the lungs of poly(I·C) mice. However, numbers of infiltrating inflammatory cells plateaued in poly(I·C)-treated mice as disease resolved while numbers increased in control mice, consistent with the histological observations shown in Fig. 8A and clinical disease progression.

Poly(I·C) is also protective when delivered intranasally at low doses, several days prior to infection, or systemically. In a recent human study, 1.6 mg poly(ICLC) [polyinosinic-poly(C) polylysinecarboxy methylcellulose], an RNase-resistant form of poly(I·C), was administered to healthy volunteers (3). Treatment resulted in an immune response that was similar to that observed after vaccination with an attenuated viral vaccine. Initially, to establish the relevance of our results to human populations, we treated mice intranasally with a dosage equivalent to that used in the human study (0.8 μg/mouse) and observed complete protection from lethal SARS-CoV infection (Fig. 9A). Further, to be useful prophylactically, poly(I·C) delivered prior to infection would need to be protective for several days. As shown in Fig. 9B, administration of poly(I·C) 3 days prior to SARS-CoV infection protected 80% of mice from lethal infection; this effect was reduced to 20 to 40% survival if poly(I·C) was delivered 5 to 10 days prior to infection. Of note, poly(I·C) treatment was effective only when initiated prior to infection; mice treated at 6 or 18 h after infection exhibited 100% mortality.

Since poly(I·C) was administered parenterally in human studies (3, 15), we treated 12- or 22-month-old mice with poly(I·C) by intraperitoneal (i.p.), intravenous (i.v.), or subcutaneous (s.c.) inoculation prior to infection with SARS-CoV (Fig. 9C) or IAV (Fig. 9D), respectively. Unlike intranasal inoculation, i.p. and i.v. delivery of 80 μg poly(I·C) resulted in mild systemic signs, including diaphoresis and transient weight loss (approximately 5%). SARS-CoV-infected 12-month-old mice were completely protected when poly(I·C) was delivered i.p. or i.v., while IAV-infected 22-month-old mice were completely protected after receiving poly(I·C) i.v. Partial protection occurred when poly(I·C) was delivered i.p. to 22-month-old IAV-infected mice.

DISCUSSION

Poly(I·C) and its analogues are approved for human use. Several phase I and phase II trials use either poly(I·C) or its RNase-resis-

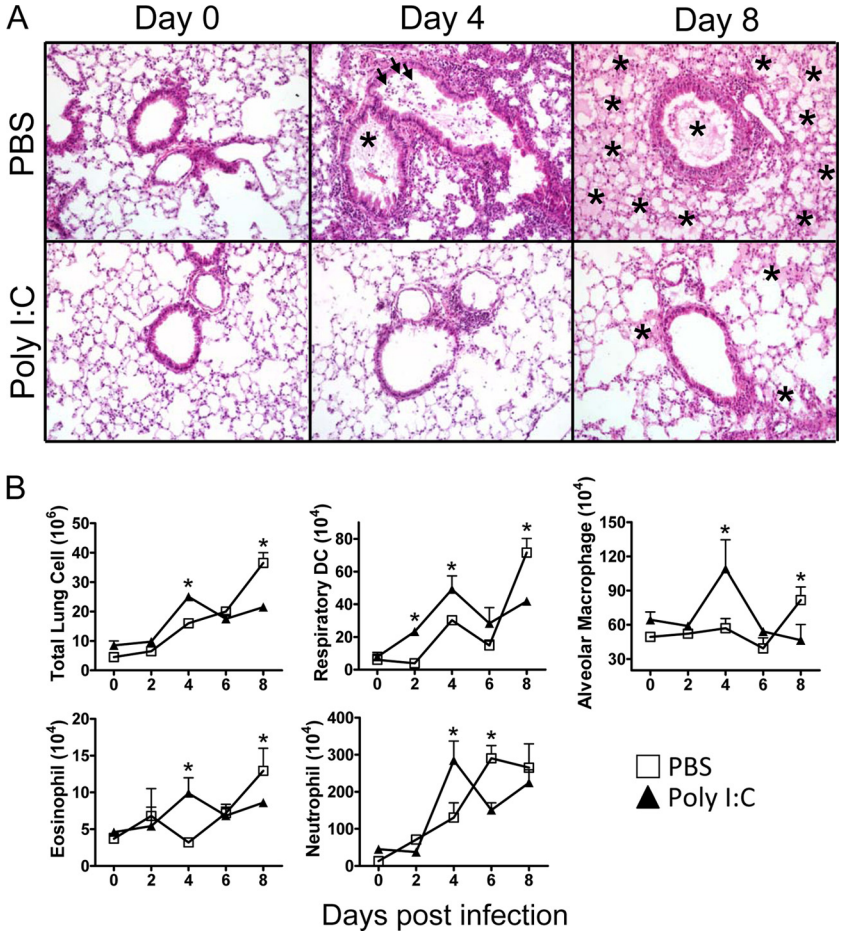

FIG 8 Earlier inflammatory cell infiltration and decreased pulmonary edema occurs in poly(I·C)-treated IAV-infected mice. Twenty-two-month-old B6 mice were treated with 20 μg poly(I·C) or PBS 48 and 6 h before intranasal infection with IAV. (A) Lungs were removed at the indicated time points p.i., fixed in zinc formalin, and embedded in paraffin. Sections were stained with hematoxylin and eosin. Asterisks indicate edema; arrows indicate necrotic debris. Two mice were analyzed at each time point in each group. (B) Lungs were harvested at the indicated time points, and after enzyme digestion, single-cell suspensions were acquired. Total numbers of lung cells, rDCs ($CD11c^+$ $MHCII^+$ $SiglecF^-$), alveolar macrophages ($CD11c^+$ $MHCII^{+/-}$ $SiglecF^+$), eosinophils ($CD45^+$ $CD11c^{+/-}$ $SiglecF^+$), and neutrophils ($CD11b^+$ $Ly6C^+$ $Ly6G^+$) in the lung are shown. $n = 3$ mice/group/time point. *, $P < 0.05$.

tant form, poly(ICLC), as an adjuvant in patients with advanced cancer (1, 15, 22). Poly(I·C) is postulated to enhance the immune response by activating dendritic cells, which results in priming and subsequent infiltration of NK and T cells with antitumor properties into tumors. Poly(I·C) treatment also augments the immune response to tumor-specific peptides, contributing to regression (26). Poly(I·C) may also be a useful adjuvant for immunization against viruses such as the H5N1 strain of IAV (13) and other pathogens.

Here, we show that intranasal treatment with TLR agonists, especially poly(I·C), is efficacious in aged animals infected with IAV or SARS-CoV. Severe IAV is characterized by high-level expression of proinflammatory cytokines and chemokines (cytokine storm) (13), which likely results from increased virus loads (4, 13, 16). The latter, in turn, may be a consequence of delayed recognition of the pathogen by the innate immune response (18). Consistent with this postulated scenario, levels of CXCL10, CCL2, IL-8, IL-6, and IL-10 correlated with virus levels and severe disease in patients infected with the H5N1 strain of IAV (4). Poly(I·C), by activating the innate immune response, would be predicted to inhibit virus replication, thereby preventing the subsequent development of a dysregulated cytokine response. Aged mice or macaques infected with SARS-CoV develop a dysregulated innate immune response to the virus (2, 25, 27) and do not develop an optimal T cell response to the virus (33) (Fig. 4). We recently showed that the deficiency in anti-SARS-CoV T cell response in aged mice resulted from the inhibitory environment present in the lung (33). Specifically, levels of the prostaglandin PGD_2 increased during aging, with levels further increased by infection with SARS-CoV or IAV (33). One consequence was decreased CCR7 expression on rDC, resulting in diminished migration to draining lymph nodes and decreased antivirus T cell priming. Treatment with PGD_2 inhibitors enhanced rDC migration and T cell responses. Poly(I·C), by activating the innate immune response, is able to prime the lung environment for a protective immune response in aged SARS-CoV-infected mice, reversing the effects of PGD_2 and other inhibitory molecules in the lungs. Protection was mediated in large part by IFN induction by TLR3-dependent and TLR3-independent pathways (Fig. 6). Most cells express TLR3 and the cytosolic RNA helicase sensors RIG-I and MDA-5, so they could be targeted by poly(I·C). We

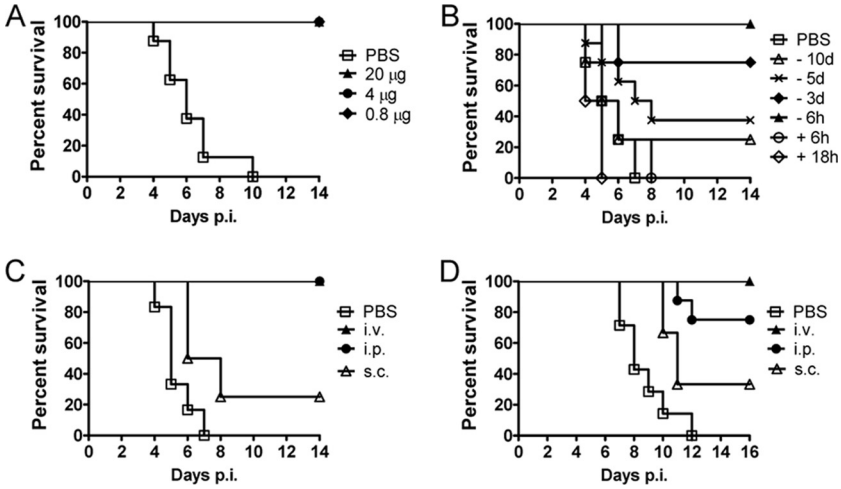

FIG 9 Poly(I·C) is protective when delivered at low doses either several days prior to infection or systemically. Twelve-month-old B6 mice were treated with various doses of poly(I·C) 6 h before infection (termed the −6-h group) with 1×10^5 PFU MA15 (A), were treated with 20 μg poly(I·C) in 50 μl PBS intranasally (the 20-μg group) at different time points before or after infection (B), or were treated with 80 μg poly(I·C) in 200 μl PBS i.p., i.v., or s.c. 6 h before infection (C). (D) Twenty-two-month-old mice were treated with 80 μg poly(I·C) in 200 μl PBS i.p., i.v., or s.c. 6 h before IAV infection. Weight loss and mortality were monitored daily. For panel A, $n = 8$ mice in the PBS group, 13 in the 20-μg group, 8 in the 4-μg group, and 8 in the 0.8-μg group. For panel B, $n = 9$ mice in the PBS group, 6 in the −10-day group, 6 in the −5-day group, 10 in the −3-day group, 8 in the −6-h group, 10 in the +6-h group, and 6 in the +18-h group. For panel C, $n = 6$ mice in the PBS group, 6 in the i.v. group, 6 in the i.p. group, and 8 in the s.c. group. For panel D, $n = 7$ mice in the PBS group, 6 in the i.v. group, 8 in the i.p. group, and 6 in the s.c. group.

showed that airway epithelial cells, which are commonly infected in SARS-CoV-infected humans and experimentally infected animals (21, 24), respond to poly(I·C) by inhibiting virus replication (Fig. 1D). Other studies suggest that endothelial cells are an important source for IFN and other cytokines and contribute to the hypercytokinemia observed in severe respiratory infections (30), so they are also likely to be targets for poly(I·C).

To be useful in human populations as a prophylactic agent in aged populations, it will be essential to deliver poly(I·C) at doses that result in no side effects and that are effective for several days after administration. Poly(I·C), delivered subcutaneously, was recently shown to induce genes associated with several innate immune pathways in human volunteers (3). The breadth of the response was very similar to that observed after immunization with the well-studied attenuated yellow fever vaccine, consistent with our results showing that poly(I·C) induces IFN-dependent and IFN-independent mechanisms of resistance. Poly(I·C) was generally well tolerated, with moderate local and mild systemic side effects reported. Our results show that poly(I·C) administered intranasally to mice is effective without obvious side effects. In contrast, mice that received poly(I·C) systemically showed mild systemic signs, consistent with the side effects observed in the human studies.

In summary, our results suggest that intranasally delivered poly(I·C) should be further investigated for prophylaxis in aged populations at high risk for severe virus respiratory infections, especially for settings like the SARS epidemic, in which no other therapeutic options are available.

ACKNOWLEDGMENTS

We thank David Meyerholz for analysis of lung sections.

This research was supported in part by grants from the NIH (RO1AI091322 [S.P.] and PO106099 [S.P. and P.B.M.]).

REFERENCES

1. **Butowski N, et al.** 2009. A phase II clinical trial of poly-ICLC with radiation for adult patients with newly diagnosed supratentorial glioblastoma: a North American Brain Tumor Consortium (NABTC01-05). J. Neurooncol. **91**:175–182.
2. **Cameron MJ, et al.** 2007. Interferon-mediated immunopathological events are associated with atypical innate and adaptive immune responses in patients with severe acute respiratory syndrome. J. Virol. **81**:8692–8706.
3. **Caskey M, et al.** 2011. Synthetic double-stranded RNA induces innate immune responses similar to a live viral vaccine in humans. J. Exp. Med. **208**:2357–2366.
4. **de Jong MD, et al.** 2006. Fatal outcome of human influenza A (H5N1) is associated with high viral load and hypercytokinemia. Nat. Med. **12**:1203–1207.
5. **Ely KH, Roberts AD, Kohlmeier JE, Blackman MA, Woodland DL.** 2007. Aging and CD8+ T cell immunity to respiratory virus infections. Exp. Gerontol. **42**:427–431.
6. **Falsey AR, Hennessey PA, Formica MA, Cox C, Walsh EE.** 2005. Respiratory syncytial virus infection in elderly and high-risk adults. N. Engl. J. Med. **352**:1749–1759.
7. **Frieman MB, et al.** 2010. SARS-CoV pathogenesis is regulated by a STAT1 dependent but a type I, II and III interferon receptor independent mechanism. PLoS Pathog. **6**:e1000849. doi:10.1371/journal.ppat.1000849.
8. **Hosking MP, Liu L, Ransohoff RM, Lane TE.** 2009. A protective role for ELR+ chemokines during acute viral encephalomyelitis. PLoS Pathog. **5**:e1000648. doi:10.1371/journal.ppat.1000648.
9. **Jia HP, et al.** 2005. ACE2 receptor expression and severe acute respiratory syndrome coronavirus infection depend on differentiation of human airway epithelia. J. Virol. **79**:14614–14621.
10. **Jiang J, et al.** 2009. Limited expansion of virus-specific CD8 T cells in the aged environment. Mech. Ageing Dev. **130**:713–721.
11. **Karp PH, et al.** 2002. An in vitro model of differentiated human airway epithelia. Methods for establishing primary cultures. Methods Mol. Biol. **188**:115–137.
12. **Katz JM, et al.** 2004. Immunity to influenza: the challenges of protecting an aging population. Immunol. Res. **29**:113–124.
13. **Kobasa D, et al.** 2007. Aberrant innate immune response in lethal infection of macaques with the 1918 influenza virus. Nature **445**:319–323.
14. **Kovacs EJ, et al.** 2009. Aging and innate immunity in the mouse: impact of intrinsic and extrinsic factors. Trends Immunol. **30**:319–324.

15. **Krown SE, Kerr D, Stewart WE, Jr, Field AK, Oettgen HF.** 1985. Phase I trials of poly(I,C) complexes in advanced cancer. J. Biol. Response Mod. **4**:640–649.
16. **Legge KL, Braciale TJ.** 2005. Lymph node dendritic cells control CD8+ T cell responses through regulated FasL expression. Immunity **23**:649–659.
17. **Meylan E, Tschopp J, Karin M.** 2006. Intracellular pattern recognition receptors in the host response. Nature **442**:39–44.
18. **Moltedo B, et al.** 2009. Cutting edge: stealth influenza virus replication precedes the initiation of adaptive immunity. J. Immunol. **183**:3569–3573.
19. **Murasko DM, Jiang J.** 2005. Response of aged mice to primary virus infections. Immunol. Rev. **205**:285–296.
20. **Nagata N, et al.** 2008. Mouse-passaged severe acute respiratory syndrome-associated coronavirus leads to lethal pulmonary edema and diffuse alveolar damage in adult but not young mice. Am. J. Pathol. **172**:1625–1637.
21. **Nicholls JM, et al.** 2006. Time course and cellular localization of SARS-CoV nucleoprotein and RNA in lungs from fatal cases of SARS. PLoS Med. **3**:e27. doi:10.1371/journal.pmed.0030027.
22. **Okada H, et al.** 2011. Induction of CD8+ T-cell responses against novel glioma-associated antigen peptides and clinical activity by vaccinations with α-type 1 polarized dendritic cells and polyinosinic-polycytidylic acid stabilized by lysine and carboxymethylcellulose in patients with recurrent malignant glioma. J. Clin. Oncol. **29**:330–336.
23. **Peiris JS, Guan Y, Yuen KY.** 2004. Severe acute respiratory syndrome. Nat. Med. **10**:S88–S97.
24. **Roberts A, et al.** 2007. A mouse-adapted SARS-coronavirus causes disease and mortality in BALB/c mice. PLoS Pathog. **3**:e5. doi:10.1371/journal.ppat.0030005.
25. **Rockx B, et al.** 2009. Early upregulation of acute respiratory distress syndrome-associated cytokines promotes lethal disease in an aged-mouse model of severe acute respiratory syndrome coronavirus infection. J. Virol. **83**:7062–7074.
26. **Seya T, Matsumoto M.** 2009. The extrinsic RNA-sensing pathway for adjuvant immunotherapy of cancer. Cancer Immunol. Immunother. **58**:1175–1184.
27. **Smits SL, et al.** 2010. Exacerbated innate host response to SARS-CoV in aged non-human primates. PLoS Pathog. **6**:e1000756. doi:10.1371/journal.ppat.1000756.
28. **Subbarao K, Roberts A.** 2006. Is there an ideal animal model for SARS? Trends Microbiol. **14**:299–303.
29. **Takeuchi O, Akira S.** 2008. MDA5/RIG-I and virus recognition. Curr. Opin. Immunol. **20**:17–22.
30. **Teijaro JR, et al.** 2011. Endothelial cells are central orchestrators of cytokine amplification during influenza virus infection. Cell **146**:980–991.
31. **Toapanta FR, Ross TM.** 2009. Impaired immune responses in the lungs of aged mice following influenza infection. Respir. Res. **10**:112.
32. **Yager EJ, et al.** 2008. Age-associated decline in T cell repertoire diversity leads to holes in the repertoire and impaired immunity to influenza virus. J. Exp. Med. **205**:711–723.
33. **Zhao J, Zhao J, Legge K, Perlman S.** 2011. Age-related increases in PGD(2) expression impair respiratory DC migration, resulting in diminished T cell responses upon respiratory virus infection in mice. J. Clin. Investig. **121**:4921–4930.
34. **Zhao J, Zhao J, Perlman S.** 2010. T cell responses are required for protection from clinical disease and for virus clearance in severe acute respiratory syndrome coronavirus-infected mice. J. Virol. **84**:9318–9325.
35. **Zhao J, Zhao J, Van Rooijen N, Perlman S.** 2009. Evasion by stealth: inefficient immune activation underlies poor T cell response and severe disease in SARS-CoV-infected mice. PLoS Pathog. **5**:e1000636. doi:10.1371/journal.ppat.1000636.
36. **Zhou H, Zhao J, Perlman S.** 2010. Autocrine interferon priming in macrophages but not dendritic cells results in enhanced cytokine and chemokine production after coronavirus infection. mBio **1**:e00219–10. doi:10.1128/mBio.00219-10.